

# A Semi-Implicit Phase Field Model for Droplet Evolution

M. H. Kazemi, D. Salac

**Abstract**—A semi-implicit phase field method for droplet evolution is proposed. Using the phase field Cahn-Hilliard equation, we are able to track the interface in multiphase flow. The idea of a semi-implicit finite difference scheme is reviewed and employed to solve two nonlinear equations, including the Navier-Stokes and the Cahn-Hilliard equations. The use of a semi-implicit method allows us to have larger time steps compared to explicit schemes. The governing equations are coupled and then solved by a GMRES solver (generalized minimal residual method) using modified Gram-Schmidt orthogonalization. To show the validity of the method, we apply the method to the simulation of a rising droplet, a leaky dielectric drop and the coalescence of drops. The numerical solutions to the phase field model match well with existing solutions over a defined range of variables.

**Keywords**—Coalescence, leaky dielectric, numerical method, phase field, rising droplet, semi-implicit method.

## NOMENCLATURE

$C$	Phase field parameter
$Ca$	Capillary number
$Ca_E$	Electric Capillary number
$Cn$	Cahn number
$E$	Electric field strength
$F$	Tension force
$f$	Electric force
$Fr$	Froude number
$L$	Characteristic length
$M$	Phase field mobility
$p$	Pressure
$Pe$	Peclet number
$R$	The radius of the droplet
$Re$	Reynolds number
$t$	Time
$t_0$	Characteristic time
$U$	Characteristic velocity
$u$	Fluid velocity
$V$	Electrical potential
$\gamma$	Surface tension
$\varepsilon$	Permittivity
$\zeta$	Interference thickness
$\mu$	Viscosity
$\rho$	Density

$\rho_E$	Free charge density
$\sigma$	Electrical conductivity
$\phi$	Chemical potential

## I. INTRODUCTION

THE numerical tracking of an interface is an important part of many physical processes simulations. There are different techniques for interface tracking, including marker particle, level set, and phase field methods. The phase field [1] is a mathematical method in which we introduce a smooth phase field function to label the two sides of an interface. In this work, the phase field is based on a solution of the Cahn-Hilliard equation, which is a result of the minimization of the free energy and is employed to describe the evolution of the phase field parameter. The phase field has mainly been applied to solidification dynamics, but it has been applied to other situations such as liquid crystal evolution, the modeling of phase transitions, polarization and electro-hydrodynamics [2], [3]. Among them, there is growing interest in the dynamic of drops in many areas such as biology, mixing, and demixing, drug delivery, separation process and atomization [4].

The semi-implicit time difference method is a method that can be used in numerical simulation model to increase the overall numerical stability. The idea is to approximate some terms implicitly and other explicitly. The goal is to allow the use of larger time steps than would be possible using an explicit scheme. Because of this reason, the semi-implicit method has been used extensively in various numerical models. Yang et al. [5] presented a robust phase field scheme to describe the pinch-off behavior of a liquid filament as well as the deformation of the consequent satellite droplet. Liu et al. [6] analyzed the mixture of fluids with a semi-discrete Fourier spectral method and exhibited various physical mechanism of model and demonstrated its robustness and versatility. Hu et al. [7] proposed the study of the coherent microstructure evolution in an elastically anisotropic system with a semi-implicit Fourier-spectral method. They illustrated that the method correctly simulates the driving force. Salac et al. [8] used a semi-implicit level set method to accurately capture the complicated behavior such as interface separation and coalescence. They showed that the proposed scheme is stable and efficient to be employed in 2D and 3D problems.

In our study, we develop a semi-implicit phase field method to simulate generic droplets. Instead of explicitly tracking the interface, we intend to implicitly capture the interface. Such a numerical model helps to provide fundamental understanding of the fluid field and the droplet deformation in developing practical applications. The method is validated with three

M. H. Kazemi is with the Department of Mechanical and Aerospace Engineering, University at Buffalo, Buffalo, NY 14260 USA (phone: 716-445-5251; fax: 716-645-2883; e-mail: mkazemi@buffalo.edu).

D. Salac is with the Department of Mechanical and Aerospace Engineering, University at Buffalo, Buffalo, NY 14260 USA (e-mail: davidsal@buffalo.edu).

example droplets: a rising drop, leaky dielectrics droplets, and coalesce of droplets in an electric field. In the first problem, the drop is driven by the buoyancy force and tension force. The second and third examples are based on leaky dielectric theory [9] and the drop is deformed by the surface tension and electric forces. In this study, the phase field is discretized by a semi-implicit method and is coupled with Navier-Stokes equation to simulate the fluid field.

## II. THEORY AND FORMULATION

### A. The Semi-Implicit Phase Field Model

The phase field model is a diffuse-interface model and is employed to study the moving interface. In this study, the domain is completely filled with two immiscible fluids and is separated by a moving interface. The domain includes the droplet and the medium fluid. The parameter  $C$  is introduced as phase field parameter to show the concentration of droplet fluid in the domain. The isocontour  $C=0.5$  represents the interface while  $C=0$  or  $C=1$  indicates the medium fluid or droplet, respectively. The phase field model is based on Cahn-Hilliard equation [1] and describes the process of phase separation. This equation can be described as:

$$\frac{\partial C}{\partial t} + u \cdot \nabla C = \nabla \cdot (M \nabla \phi), \quad (1)$$

where  $u$  is the fluid velocity,  $M$  is the phase field mobility, and  $\phi$  is the chemical potential. The chemical potential is the rate of total free energy with respect to  $C$  which is  $\phi = \partial f / \partial C$  as

$$f(C) = \frac{1}{2} \xi \gamma \alpha |\nabla C|^2 + \zeta^{-1} \gamma \alpha \frac{1}{4} C^2 (1-C)^2, \quad (2)$$

where  $\alpha$  is constant and equal to  $6\sqrt{2}$ ,  $\gamma$  is the surface tension, and  $\zeta$  presents the interface thickness. Let the characteristic length,  $R$ , be the radius of a spherical droplet with the same enclosed volume. Given the characteristic time  $t_0$ , the characteristic velocity is expressed by  $U = R / t_0$ . The notation \* denotes a non-dimensional variable (i.e.  $u^* = u / U$  and  $t^* = t / t_0$ ). The Cahn-Hilliard equation is non-dimensionalized based on the velocity  $u = U u^*$  and  $t = t^* R / U$ , chemical potential  $\phi = \phi^* \beta$  in which  $\beta = \zeta^{-1} \gamma \alpha$ . By scaling the equation, we reach to the following,

$$\frac{\partial C}{\partial t^*} + u^* \cdot \nabla C = \frac{\alpha}{Pe} \nabla^2 \cdot \left( \frac{1}{2} (2C^3 - 3C^2 + C) - C n^2 \nabla^2 C \right). \quad (3)$$

Based on the non-dimensionalization process, the following parameters are produced,

$$Pe = \frac{RU\zeta}{M\gamma} \quad \text{and} \quad C_n = \frac{\zeta}{R}.$$

In the right hand side of (3), the first term forces the system to phase segregate and the second term tries to minimize the gradient energy of the interface. In a fully implicit scheme, such as the implicit Euler scheme (backward Euler), we would be required to solve a system of nonlinear equation at every time step, which would be computationally expensive. In this study, a semi-implicit time scheme is presented to solve the phase field equation. It can be shown that the semi-implicit discretization gives us a robustness in time. In this method, we defined the linear contribution implicitly and the non-linear contributions explicitly. Solving the equation by applying the semi-implicit method and first order time integration, we obtain the following discrete form

$$\frac{C^{n+1} - C^n}{\Delta t} + u^n \cdot \nabla C^n = \frac{\alpha}{Pe} \nabla^2 \cdot \left( \frac{1}{2} (2C^3 - 3C^2 + C) - C n^2 \nabla^2 C^{n+1} \right). \quad (4)$$

The subscript  $n$  refers to the solution at the previous time step. Given the  $u^n$  and  $C^n$ , the objective is to solve for  $C^{n+1}$  and use that result in order to obtain the  $u^{n+1}$  by solving the flow fluid equations. Equation (4) can be expressed as

$$C^{n+1} + \frac{\alpha \Delta t}{Pe} C n^2 \nabla^2 C^{n+1} = C^n - \Delta t \bar{u}^n \cdot \nabla C^n + \frac{\alpha \Delta t}{2Pe} \nabla^2 \cdot (2C^3 - 3C^2 + C)^n. \quad (5)$$

The spatial derivatives are discretized with a second order accurate central difference scheme and coupled with the fluid flow equation to get the velocity and solved to obtain the next phase field parameter in time and the new location of interface.

After discretization, the whole equation can be written in the form of  $Ax = b$ , where  $A$  is the coefficient matrix,  $x$  the unknown phase field parameter, and  $b$  the right hand side vector in (5). This linear system can be solved with a matrix-free iterative linear system solution method, and in this, the GMRES solver (Generalized minimal residual method) using modified Gram-Schmidt orthogonalization is utilized.

### B. The Fluid Motion Equation and Projection Method

We now present the governing equations for the incompressible fluid. Based on the physics of problem, the momentum equation is used with a phase-field dependent surface force. In addition, we employ the buoyancy force in the first example and the electric force in second and third example to validate the methods. The Navier-Stokes and mass conservative equations take the form of

$$\rho(C) \left( \frac{\partial u}{\partial t} + u \cdot \nabla u \right) = \nabla \cdot p + \nabla \cdot (\mu(C) (\nabla u + \nabla u^T)) + f_j + f_e + f_g, \quad (6)$$

$$\nabla \cdot u = 0. \quad (7)$$

Since the density  $\rho(C)$  and viscosity  $\mu(C)$  change across the interface, they depend on the phase parameter  $C$  and they

are as

$$\rho(C) = \rho_1 C + \rho_2 (1 - C) \text{ and } \mu(C) = \mu_1 C + \mu_2 (1 - C). \quad (8)$$

The notation 1 and 2 stands for the fluid property of droplet and medium fluid, respectively. In (6),  $p$  is the pressure,  $f_e$  is the electric force,  $f_y = -C\nabla\phi$  is the surface tension force and  $f_g = (\rho - \rho_2)g$  stands for the buoyancy force. In addition, the superscript  $T$  stands for the transpose operator. In the present study, the leaky dielectric model presented by Saville [9] is used to obtain the electric force. The leaky dielectric fluid can be expressed by

$$\nabla \cdot (\sigma(C)E) = 0. \quad (9)$$

The electric field in (9) is  $E = -\nabla V$  where  $V$  is the electrical potential, and  $\sigma(C)$  is the electrical conductivity, which changes based on the property of fluid and depends on parameter  $C$ . The Poisson equation, (9), is solved to obtain the electrical potential. As mentioned, the electric field is assumed to be irrotational, therefore, the electric force acting on the interface of droplet can be expressed as [9]

$$f = \int (\rho_e E - \frac{1}{2} E^2 \nabla \varepsilon(C)) dx^3, \quad (10)$$

where  $\varepsilon(C)$  stands for the permittivity of two phases and is determined by using a similar expression to the fluid conductivity, and  $\rho_e$  is the free charge density. Gauss's Law gives the free charge density as:

$$\rho = \nabla \cdot (\varepsilon(C)E). \quad (11)$$

By having the electrical field from (9), the electrical force can be obtained.

We now describe the discretization of the fluid equation and we used the notation  $*$  for nondimensional variables (i.e.  $\mu^* = \mu / \mu_2$  and  $\rho^* = \rho / \rho_2$ ). The normalized equation is based on the density  $\rho = \rho^* \rho_2$ , viscosity  $\mu = \mu^* \mu_2$ , and pressure  $p = p^* \rho_2 U^2$ . In the leaky dielectric problem, the electric field at the boundaries is imposed as  $E = E^* E_0 = E^* V_0 / L$  where  $E^*$  is the normalized strength of the applied electric field and  $E_0$  is the strength of electric field, given by  $6V_0$  which is the drop of electrical potential between two electrodes separated by a length of  $6L$ . The electric permittivity is defined as  $\varepsilon = \varepsilon^* \varepsilon_2 \varepsilon_0$  in which  $\varepsilon^*$  is normalized permittivity and  $\varepsilon_2 \varepsilon_0$  is dielectric permeability of the outer fluid [9], and the electric conductivity is expressed as  $\sigma = \sigma^* \sigma_2$  in which  $\sigma^*$  is normalized conductivity. We express the non-dimensionalized fluid flow equation as follows

$$\rho^*(C) \left( \frac{\partial u^*}{\partial t^*} + u^* \cdot \nabla u^* \right) = -\nabla p^* + \frac{1}{\text{Re}} \nabla \cdot (\mu^*(C) (\nabla u^* + \nabla u^{*T})) - \frac{1}{\text{Re} Ca Cn} C \nabla \phi^* + \frac{Ca_e}{\text{Re} Ca} \frac{R}{L} f_e^* + \frac{1}{Fr^2} (\rho^* - 1) \hat{g}. \quad (12)$$

The dimensionless parameters Reynolds number  $\text{Re}$ , Capillary number  $Ca$ , Electric Capillary number  $Ca_e$ , and Froude number  $Fr$  are as,

$$\text{Re} = \frac{\rho_2 UR}{\mu_2}, \quad Ca = \frac{\mu_2 U}{\gamma}, \quad Ca_e = \frac{\varepsilon^* \varepsilon_2 E_0^2 R}{\gamma} \text{ and } Fr = \frac{U}{\sqrt{Rg}}.$$

For the leaky dielectric fluid, the electric force is normalized as,

$$f_e^* = \nabla \cdot (\varepsilon^*(C) E^*) E^* - \frac{1}{2} E^{*2} \nabla \varepsilon^*(C). \quad (13)$$

We used a projection method to solve the Navier-Stokes equation. The first step is to use a semi-implicit scheme in time in order to obtain an intermediate velocity field  $\hat{u}$ . Thus, the equation can be expressed as:

$$\rho(C^n) \left( \frac{\hat{u} - u^n}{\Delta t} + u^n \cdot \nabla u^n \right) = -\nabla p^n + \frac{1}{\text{Re}} \nabla \cdot (\mu(C^n) (\nabla \hat{u} + \nabla u^{nT})) - \frac{1}{\text{Re} Ca Cn} f_y^n + \frac{Ca_e}{\text{Re} Ca} \frac{R}{L} f_e^n + \frac{1}{Fr^2} f_g^n. \quad (14)$$

The superscript  $n$  refers to the solution at the previous time step. In order to obtain the intermediate velocity, the following equation is solved.

$$(\rho(C^n) - \frac{\Delta t}{\text{Re}} \nabla \cdot (\mu(C^n) \nabla)) \hat{u} = R.H.S., \quad (15)$$

which is a linear equation of  $\hat{u}$ , and the right hand side of the equation is expressed as

$$\rho(C^n) u^n + \Delta t (-u \cdot \nabla u - \nabla p^n + \frac{1}{\text{Re}} \nabla \cdot (\mu(C^n) \nabla u^{nT})) - \frac{1}{\text{Re} Ca Cn} f_y^n + \frac{Ca_e}{\text{Re} Ca} \frac{R}{L} f_e^n + \frac{1}{Fr^2} f_g^n. \quad (16)$$

It is worth pointing out that the convective term in the fluid flow equation is discretized by a first order upwinding scheme and the viscous term is discretized with a second order accurate central finite difference scheme. After discretization, the whole equation can be written in the form of  $Ax = b$ , where  $A$  coefficient matrix,  $x$  the unknown intermediate velocity field vector and vector  $b$  is equal to (16). As before, the GMRES solver (Generalized minimal residual method) is employed to solve the linear system.

In the second half of the algorithm, the projection step, we use the intermediate velocity to obtain the delta pressure which is used to correct the pressure of the system.

$$\rho(C^n) \left( \frac{u^{n+1} - \hat{u}}{\Delta t} \right) = -\nabla p' \quad (17)$$

The final velocity  $u^{n+1}$  is divergence free so  $\nabla \cdot u^{n+1} = 0$  and the following equation is derived,

$$\nabla \cdot \left( \frac{1}{\rho(C^n)} \nabla p' \right) = \frac{\nabla \cdot \hat{u}}{\Delta t} \quad (18)$$

The density  $\rho(C)$  depends on the phase parameter  $C$  and it can be discretized with the help of harmonic interpolation, which gives a good approximation over the interface when the density difference is high. The harmonic interpolation of density is expressed as

$$\frac{1}{\rho_{i+1/2}} = \frac{1}{2} \left( \frac{1}{\rho_i} + \frac{1}{\rho_{i+1}} \right) \quad (19)$$

After discretization of (18), it can be written in the form of  $Ax = b$ , where  $A$  coefficient matrix,  $x$  the unknown  $p'$  vector, and  $b$  is right hand side in the equation. By solving the linear system using the generalized minimal residual method for  $p'$ , the final corrected velocity and pressure get the form,

$$u' = -\frac{\Delta t}{\rho(C)} \nabla p', \quad (20)$$

$$u^{n+1} = u^n + u' \quad \text{and} \quad p^{n+1} = p^n + p'. \quad (21)$$

### C. Algorithm of Computation

The summarization of the computation is as follows

- Step 1: Use (5), to compute  $C^{n+1}$
- Step 2: Use (9), to compute  $V$ , if needed.
- Step 3: Use (14), to calculate  $\hat{u}$
- Step 4: Using (18) to (21), to compute  $p^{n+1}$  and  $u^{n+1}$
- Step 5: Advance one time step and return to step 1 until the error condition for velocity is satisfied in the whole domain.

## III. NUMERICAL SIMULATION

In this section, we present numerical simulations using our semi-implicit phase field method. We simulate three examples: a rising droplet, a leaky dielectric droplet, and the coalescence of droplets in an electric field. The driving forces are gravity and surface tension in the rising droplet simulation and the electric force and surface tension in the leaky dielectric droplet and coalescence of multi drops. As shown in Fig. 1, we describe an oblate shape as when the major axis of the droplet is parallel to the  $x$  axis, while a prolate shape is the case where the major axis is in the  $y$  direction.

In the following numerical simulations, the density, viscosity, electrical permittivity, and conductivity ratio of the two fluids are presented as  $\lambda_\rho = \rho_1 / \rho_2$ ,  $\lambda_\mu = \mu_1 / \mu_2$ ,

$\lambda_\epsilon = \epsilon_1 / \epsilon_2$ , and  $\lambda_\sigma = \sigma_1 / \sigma_2$ , respectively. We will examine the method and validate our result with the existing solutions solved by other methods. The equations are discretized on a Cartesian mesh. Two choices exist in Cartesian meshes: Collocated mesh and Staggered mesh. A collocated mesh is employed to simulate droplets as it allows us to have all variables at the same point in space.

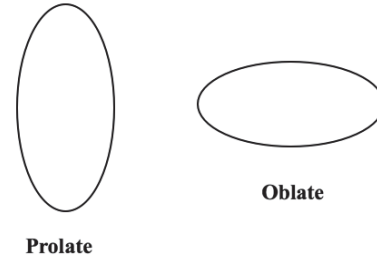


Fig. 1 The prolate and oblate droplet and their orientations with regard to the direction of the field

### A. Rising Droplet

In this numerical solution, we consider the movement of a rising droplet with different radius in a domain with a size of [6Rx6R]. In this case, we have periodic boundary conditions for both directions. Periodic boundary conditions are often chosen for approximating a large system by using a small part called unit cell. The schematic figure of unit cell is shown in Fig. 2.

The droplet is labeled as liquid 1 and the exterior fluid is labeled as liquid 2. We applied the parameter of liquid 2 for the dimensionless parameter and radius of droplet  $R$  for the characteristic parameter. As expressed, the phase field parameter is  $C = 1$  for the droplet and  $C = 0$  for the rest of the domain. For the selected domain the non-dimensional parameters are chosen as  $Re = 1$ ,  $Ca = 0.2$ ,  $Pe = 1800$ ,  $Cn = 0.025$ ,  $Fr = 1$ ,  $Ca_E = 0$ ,  $\lambda_\rho = 0.5$ , and  $\lambda_\mu = 0.5$ . The mesh size for this simulation is set to 256x256.

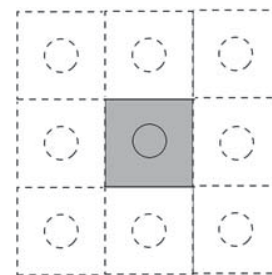


Fig. 2 Schematic illustration of the periodic unit cell for a rising droplet

For validation of our phase field, the effect of surface tension alone on droplet is done, while the buoyancy force is ignored. A detailed interface study is presented in Fig. 3 for an initially prolate shape with a semi-axis length of  $R_a = R$  in the  $x$  direction and  $R_b = 1.5R$  in the  $y$  direction. It is expected that final shape equilibrium shape is circular.

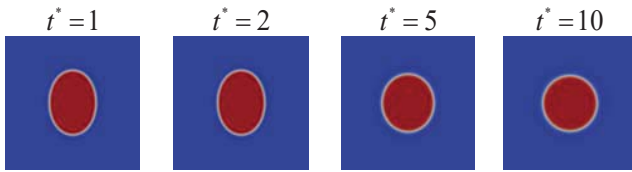


Fig. 3 Droplet deformation under the effect of surface tension force alone. The initial shape is a prolate and the equilibrium shape is circular. Shown for  $t^* = 1, 2, 5$  and  $10$

Fig. 4 shows the droplet deformation over time under the combined effects of surface tension and the buoyancy force. The initial droplet radius is  $0.5R$ . As shown in the figure, the droplet starts to rise at a small velocity. But, when time goes by, we can see the increase in the rise velocity. Since we have a small radius, the interface is largely unaffected due to the strong surface tension effects.

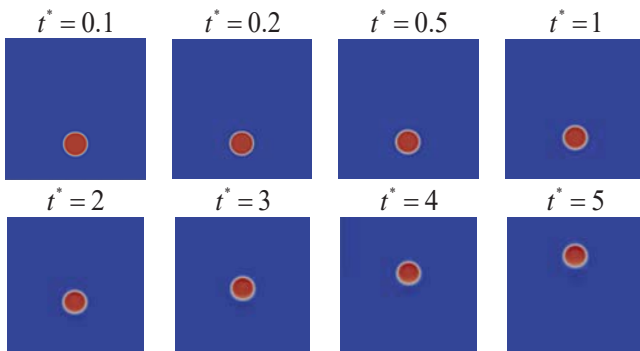


Fig. 4 Droplet deformation under the effect of surface tension and gravity, the initial shape is circular with a radius of  $0.5r$ . Shown at  $t^* = 0.1, 0.2, 0.5, 1, 2, 3, 4$  and  $5$

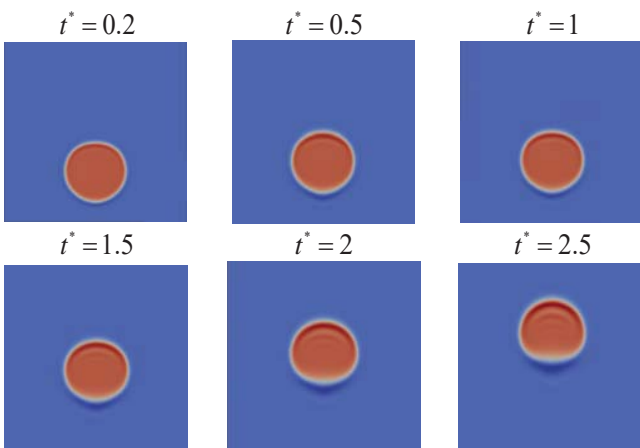


Fig. 5 Droplet deformation under the effect of surface tension and gravity, the initial shape is circular with a radius of  $R$ . Shown at  $t^* = 0.1, 0.2, 0.5, 1, 2, 3, 4$  and  $5$

Droplet deformation over time for an initial radius of  $R$  is shown in Fig. 5. As shown, we have slight deformation of the interface. The larger radius causes lower tension forces, which allows for more interface deformation. The droplet tends to be disk-like when it moves upward and it agrees well with the

work by Inamuro et al. [10] and Liu et al. [6]. As before, the droplet starts to rise at a small velocity, but as time goes by, we can see the increase in the rise velocity.

### B. Leaky Dielectric

In this numerical solution, we consider the combined effect of surface tension and electrical forces while the buoyancy force is ignored. The initial shape of the droplet in each simulation is circular. The domain size is  $[6R \times 6R]$  while  $R$  is the radius of the droplet. The top and bottom of the domain are infinite walls with no slip boundary conditions for velocity and Neumann for the pressure. A Neumann boundary condition is used on top and down for the phase field parameter  $C$ . The non-dimensional electric potential is set to be  $V = 6V_0$  on the top and  $V = 0$  at the bottom of the domain. Periodic boundary conditions are used at the left and right boundaries. A schematic figure of the domain is shown in Fig. 6. The mesh size is chosen to be  $257 \times 257$ .

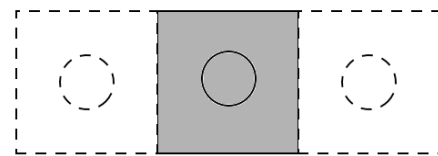


Fig. 6 Schematic illustration of the periodic unit cell for a droplet in an electric field

For validation, we compared the small droplet deformation with an analytical prediction by Taylor [11]. The label of the fluid is similar to the rising droplet. In the following study, the droplet and medium fluid has the same viscosity and density,  $\lambda_p = 1$  and  $\lambda_u = 1$ , but there is a conductivity and emissivity difference between them. The non-dimensional parameters are  $Re = 1$ ,  $Ca = 0.2$ ,  $Pe = 1800$ ,  $Cn = 0.025$ , and  $Ca_E = 0.2$  while the buoyancy force is ignored. Let  $L$  and  $B$  be the parallel and perpendicular axis length of the ellipsoid with respect to the applied electric field. Using the Taylor theory [11], the final shape of droplet can be predicted by

$$D = \frac{L-B}{L+B} = \frac{9Ca_E f_d(\sigma_1/\sigma_2, \epsilon_1/\epsilon_2, \mu_1/\mu_2)}{16(2 + \sigma_1/\sigma_2)^2} \quad (22)$$

The function,  $f_d(\sigma_1/\sigma_2, \epsilon_1/\epsilon_2, \mu_1/\mu_2)$ , represents the discriminating function,

$$f_d\left(\frac{\sigma_1}{\sigma_2}, \frac{\epsilon_1}{\epsilon_2}, \frac{\mu_1}{\mu_2}\right) = \left(\frac{\sigma_1}{\sigma_2}\right)^2 + 1 - 2\frac{\epsilon_1}{\epsilon_2} + \frac{3}{5}\left(\frac{\sigma_1 - \epsilon_1}{\sigma_2 - \epsilon_2}\right)\frac{2 + 3\mu_1/\mu_2}{1 + \mu_1/\mu_2} \quad (23)$$

where the droplet takes a shape of spheroid for  $f_d = 0$ , a prolate shape for  $f_d < 0$  and an oblate shape for  $f_d > 0$ .

Fig. 7 shows the comparison of deformation between our numerical simulation and Taylor's theory for small deformation. All simulations are performed until a time  $t^* = 20$  to reach the steady state. The conductivity ratio,  $\lambda_\sigma$ , is

varied while the emissivity ratio is fixed at  $\lambda_e = 2$ . The results show good agreement with Taylor's Theory and it can be concluded that our numerical simulation predicts the electrical forces well in a leaky dielectric droplet.

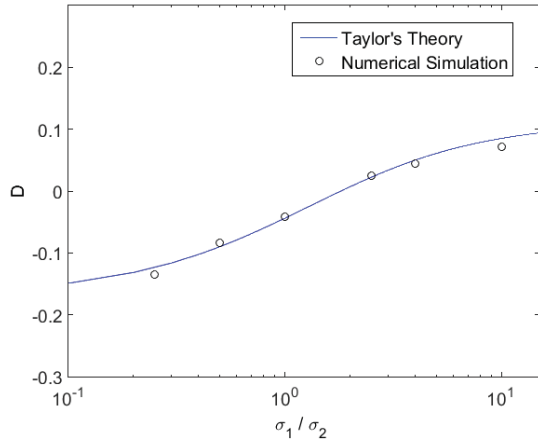


Fig. 7 Comparison of deformation between numerical results and Taylor's theory for  $\lambda_e = 2$

In the next study, the single deformation of a leaky dielectric droplet is investigated. Fig. 8 shows the equilibrium deformation of droplets with at the same conductivity ratio and two emissivity ratios. As shown in Fig. 8, when  $\lambda_\sigma = 5$  and  $\lambda_e = 0.5$ , the spherical droplet starts to deform, and at  $t^* = 20$  it relaxes to the prolate shape, and thus  $D > 0$ . In addition, when  $\lambda_\sigma = 5$  and  $\lambda_e = 50$ , the final deformation relaxes to oblate shape after  $t^* = 20$ , and thus  $D < 0$ . Our simulation showed a good agreement with Taylor's theory. In each shape, there are four vortices inside and four vortices outside which are opposite to each other in oblate and prolate shape, and have been observed previously [12].

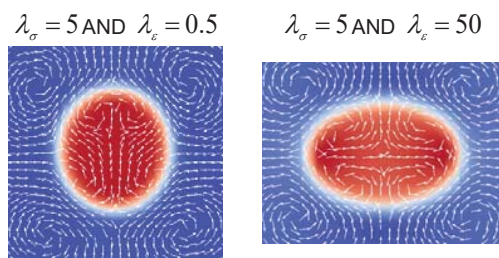


Fig. 8 A leaky droplet in a DC electric field

### C. Leaky Dielectric

The phenomenon of a dielectric droplet or particle moving in a non-uniform electric field is referred to as dielectrophoresis [13]. The combination of four droplets is selected to demonstrate the applicability of the semi-implicit phase field method.

Fig. 9 shows the coalescence of four droplets in an electric field at  $t^* = 0, 5, 20, 30, 40, 100, 200, 205, 210, 215, 220$ , and 240. The initial distances between spherical droplets are  $R$  in

the vertical direction and  $0.5R$  in horizontal direction. The electric field is applied vertically, while the parameters are the same as those in the single droplet example, shown previously.

As shown in Fig. 9, the coalescence starts in the direction normal to the electric field. As the droplets evolve into an oblate shape, they collide and merge. After coalescence, the remaining two droplets begin to attract each other. Thus, because of electric force and circulatory motion, the final coalescence happens. This example agrees well with the work by Yang et al. [14].

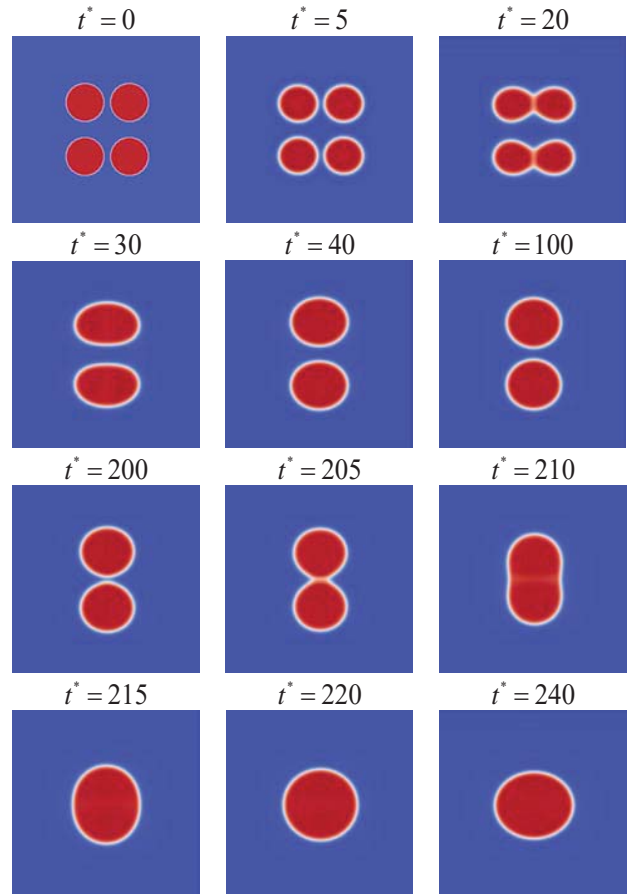


Fig. 9 Coalescence of four leaky droplets in electric field at times  $t^* = 0.5, 20, 30, 40, 100, 200, 205, 210, 215, 220$  and 240 where  $\lambda_\sigma = 0.25$  and  $\lambda_e = 2$

## IV. CONCLUSION

A semi-implicit phase field method has been developed for the numerical solution of droplets. The method can simulate two-phase flow by combining the Cahn-Hilliard phase field equation with the Navier-Stokes equations. We have shown that our semi-implicit phase field method can be applied to a wide range of examples and driving forces including buoyancy, surface tension, and electric forces. In this study, the Navier-Stokes equation and phase field methods are coupled numerically and solved by a GMRES solver. Special advantages of this method are that it can be used with larger time steps than explicit schemes and it relatively easy to

implement. To validate the method, we implement three two-phase field examples including a rising droplet, a leaky dielectric droplet, and the coalescence of multiple drops. In the simulation of rising droplet, the results show that the deformation of interface tends to be disk-like when it moves upward which shows a good match with previous reported results. In the leaky dielectric example, a comparison of results for small deformation with the Taylor's theory shows the method has good accuracy when predicting the electric force. Employing the method for coalescence of four drops, they deformed into an oblate shape. The droplets then collide and merge together in x direction. Due to the electric force and circulatory motion, the two big drops gradually moved together in y direction to coalescence to a single drop.

and engineering interests are focused on Computational Fluid Mechanics, Design Engineering, Heat Transfer, Fluid Mechanics, Nano-Fluids, Heating, Ventilation and Air Conditioning and Heat Exchangers.

He has conducted and been involved on several projects sponsored by companies such as Delfingen, Entekhab Industrial Group and ICTI (Information and Communication Technology Institute). He is a recipient of Graduate Student Competitive Scholarship Award from University at Buffalo. He is a member of some of the most remarkable honorary societies of United States such as ASME (American Society of Mechanical Engineers) and ASHRAE (American Society of Heating, Refrigeration, and Air-Conditioning Engineers).

#### REFERENCES

- [1] J. W. Cahn and J. E. Hilliard, "Free energy of a nonuniform system. I. Interfacial free energy," *The Journal of chemical physics*, vol. 28, 1958, pp. 258-267.
- [2] W. Boettinger, J. Warren, C. Beckermann, and A. Karma, "Phase-field simulation of solidification 1," *Annual review of materials research*, vol. 32, 2002, pp. 163-194.
- [3] L.-Q. Chen, "Phase-field models for microstructure evolution," *Annual review of materials research*, vol. 32, 2002, pp. 113-140.
- [4] J. Hua, L. K. Lim, and C.-H. Wang, "Numerical simulation of deformation/motion of a drop suspended in viscous liquids under influence of steady electric fields," *Physics of Fluids (1994-present)*, vol. 20, 2008, p. 113302.
- [5] X. Yang, J. J. Feng, C. Liu, and J. Shen, "Numerical simulations of jet pinching-off and drop formation using an energetic variational phase-field method," *Journal of Computational Physics*, vol. 218, 2006, pp. 417-428.
- [6] C. Liu and J. Shen, "A phase field model for the mixture of two incompressible fluids and its approximation by a Fourier-spectral method," *Physica D: Nonlinear Phenomena*, vol. 179, 2003, pp. 211-228.
- [7] S. Hu and L. Chen, "A phase-field model for evolving microstructures with strong elastic inhomogeneity," *Acta materialia*, vol. 49, 2001, pp. 1879-1890.
- [8] D. Salac and W. Lu, "A local semi-implicit level-set method for interface motion," *Journal of Scientific Computing*, vol. 35, 2008, pp. 330-349.
- [9] D. Saville, "Electrohydrodynamics: The Taylor-Melcher leaky dielectric model," *Annual review of fluid mechanics*, vol. 29, 1997, pp. 27-64.
- [10] T. Inamuro, T. Ogata, S. Tajima, and N. Konishi, "A lattice Boltzmann method for incompressible two-phase flows with large density differences," *Journal of Computational Physics*, vol. 198, 2004, pp. 628-644.
- [11] G. Taylor, "Studies in electrohydrodynamics. I. The circulation produced in a drop by electrical field," in *Proceedings of the Royal Society of London A: Mathematical, Physical and Engineering Sciences*, 1966, pp. 159-166.
- [12] Y. Lin, P. Skjetne, and A. Carlson, "A phase field model for multiphase electro-hydrodynamic flow," *International Journal of Multiphase Flow*, vol. 45, 2012, pp. 1-11.
- [13] J. Baygents, N. Rivette, and H. Stone, "Electrohydrodynamic deformation and interaction of drop pairs," *Journal of Fluid Mechanics*, vol. 368, 1998, pp. 359-375.
- [14] Q. Yang, B. Q. Li, and Y. Ding, "3D phase field modeling of electrohydrodynamic multiphase flows," *International Journal of Multiphase Flow*, vol. 57, 2013, pp. 1-9.

**M.H. Kazemi** is a researcher in the fields of Thermal-Fluid Sciences and Design Engineering at University at Buffalo. He has dual Master of Science degrees in Mechanical Engineering from University of Tehran, IRAN and University at Buffalo, USA. He has published several papers, which gained notable worldwide attention. Many other scientists at different institutes and different projects have used the results of his research, globally. His research